A Miniaturized, Programmable Pacemaker for Long-Term Studies in the Mouse

Maarten Hulsmans,* Aaron D. Aguirre,* Matthew D. Bonner, Aneesh Bapat, Sebastian Cremer, Yoshiko Iwamoto, Kevin R. King, Filip K. Swirski, David J. Milan, Ralph Weissleder, Matthias Nahrendorf

Rationale: **Cardiac pacing is a critical technology for the treatment of arrhythmia and heart failure. The impact of specific pacing strategies on myocardial function is an area of intense research and high clinical significance. Mouse models have proven extremely useful for probing mechanisms of heart disease, but there is currently no reliable technology for long-term pacing in the mouse.**

Objective: **We sought to develop a device for long-term pacing studies in mice. We evaluated the device for (1) treating third-degree atrioventricular block after macrophage depletion, (2) ventricular pacing-induced cardiomyopathy, and (3) high-rate atrial pacing.**

Methods and Results: **We developed a mouse pacemaker by refashioning a 26 mm×6.7 mm clinical device powered by a miniaturized, highly efficient battery. The electrode was fitted with a single flexible lead, and custom software extended the pacing rate to up to 1200 bpm. The wirelessly programmable device was implanted in the dorsal subcutaneous space of 39 mice. The tunneled lead was passed through a left thoracotomy incision and attached to the epicardial surface of the apex (for ventricular pacing) or the left atrium (for atrial pacing). Mice tolerated the implantation and both long-term atrial and ventricular pacing over weeks. We then validated the pacemaker's suitability for the treatment of atrioventricular block after macrophage depletion in *Cd11b*^{DTR} mice. Ventricular pacing increased the heart rate from 313±59 to 550 bpm (P<0.05). In addition, we characterized tachypacing-induced cardiomyopathy in mice. Four weeks of ventricular pacing resulted in reduced left ventricular function, fibrosis, and an increased number of cardiac leukocytes and endothelial activation. Finally, we demonstrated the feasibility of chronic atrial pacing at 1200 bpm.**

Conclusions: **Long-term pacing with a fully implantable, programmable, and battery-powered device enables previously impossible investigations of arrhythmia and heart failure in the mouse. (*Circ Res*. 2018;123:1208-1219. DOI: 10.1161/CIRCRESAHA.118.313429.)**

Key Words: artificial pacemaker ■ atrial fibrillation ■ atrioventricular block ■ cardiac arrhythmia ■ heart failure ■ inflammation ■ mice

Cardiac pacing therapies play an essential role in the modern treatment of many forms of clinical heart disease. For bradyarrhythmias resulting from dysfunction of the sinus node or the atrioventricular node, implantable pacemakers are life-sustaining devices that can return patients to a normal quality of life.[1] Biventricular pacing for cardiac resynchronization has also gained importance in the management of heart failure with reduced left ventricular (LV) function and left bundle branch conduction abnormality.[2] Because not all patients respond to cardiac pacing in the same way, many important biological questions about the underlying mechanisms of pacing-induced cardiomyopathy and cardiac resynchronization therapies remain open.[3] This highlights the potential for future innovations in pacing techniques that may improve clinical outcomes.

In This Issue, see p 1177
Meet the First Author, see p 1178

Mouse models of cardiac arrhythmia, heart failure, and cardiac pacing are critical to uncovering underlying mechanisms of disease and to understand the susceptibility of various genetic manipulations to arrhythmia. Mice allow complex genetic manipulation, disease modeling, and molecular investigations that are difficult, if not impossible, to replicate in larger animals. In addition, experiments can be done at lower cost and higher

In September 2018, the average time from submission to first decision for all original research papers submitted to *Circulation Research* was 14.06 days.

From the Department of Radiology, Center for Systems Biology (M.H., A.D.A., S.C., Y.I., K.R.K., F.K.S., R.W., M.N.), Cardiology Division (A.D.A., D.J.M.), Cardiovascular Research Center (A.B., D.J.M., M.N.), Massachusetts General Hospital and Harvard Medical School, Boston; Cardiology Division, Brigham and Women's Hospital and Harvard Medical School, Boston, MA (A.B.); Department of Systems Biology, Harvard Medical School, Boston, MA (R.W.); Cardiac Rhythm and Heart Failure, Medtronic PLC, Mounds View, MN (M.D.B.); Department of Bioengineering, Jacobs School of Engineering (K.R.K.) and Department of Medicine, Cardiology Division (K.R.K.), University of California San Diego, La Jolla; and Program in Population and Medical Genetics, The Broad Institute of Harvard and MIT, Cambridge, MA (D.J.M.).

*These authors contributed equally to this article.

The online-only Data Supplement is available with this article at https://www.ahajournals.org/doi/suppl/10.1161/CIRCRESAHA.118.313429.

Correspondence to Matthias Nahrendorf, MD, PhD, Department of Radiology, Center for Systems Biology, Massachusetts General Hospital and Harvard Medical School, Simches Research Building, Room 8–226, 185 Cambridge St, Boston, MA 02114. Email mnahrendorf@mgh.harvard.edu

Novelty and Significance

What Is Known?

- Implantable cardiac pacing devices are essential for the treatment of many forms of clinical heart disease, but long-term pacing can also induce adverse cardiac remodeling.
- Mouse models have proven extremely useful for uncovering pathways leading to heart disease.
- There is currently no reliable technology available for long-term pacing in freely moving mice.

What New Information Does This Article Contribute?

- We developed a fully implantable, programmable mouse pacemaker with a highly efficient battery enabling long-term ventricular and atrial pacing studies in mice.
- In ventricular configuration, the mouse pacemaker is suitable for treatment and examination of complete heart block and for studying chronic tachypacing-induced cardiomyopathy characterized by reduced left ventricular function, fibrosis, and myocardial inflammation.
- Chronic high-rate atrial pacing does not lead to reduced ventricular function but may predispose mice to atrial fibrillation.

Cardiac pacemakers are life-sustaining devices used for the treatment of arrhythmia and heart failure. However, long-term pacing in patients can also induce adverse cardiac remodeling leading to pacing-induced cardiomyopathy. Development of implantable pacing devices for mice is essential to study pathomechanisms of conduction system disorders and heart failure, but prior efforts to engineer devices appropriate for cardiac pacing in mice were limited with respect to pacing duration and scalability. We developed a small form factor, low-weight device with durable lead design and extended battery life, enabling continuous ventricular and atrial pacing for weeks. We used the device for ventricular pacing to successfully treat third-degree atrioventricular block in mice after macrophage depletion and to probe underlying mechanisms of chronic tachypacing-induced cardiomyopathy. We also demonstrated its use for examining long-term atrial pacing at a high rate. The developed pacemaker device opens up new opportunities to study arrhythmias and heart failure in the mouse.

Nonstandard Abbreviations and Acronyms

Bnp	brain natriuretic peptide
Ccl2	chemokine (C-C motif) ligand 2
Col1a2	collagen type I alpha 2
Col3a1	collagen type III alpha 1
DT	diphtheria toxin
Icam1	intercellular adhesion molecule 1
LV	left ventricular
Opn	osteopontin
Tgfb1	transforming growth factor beta 1

throughput. Cardiac pacing strategies have been used in larger animals to develop models of atrial fibrillation or sudden death,[4,5] but similar approaches have not been possible to test in mice because of the lack of available technologies for chronic pacing in these small animals.[3] The ability to pace genetically modified mice will enable many important investigations in the field of cardiac electrophysiology and heart failure.[3] Prior attempts to create fully implantable pacemakers for mice have been limited to <1 week in pacing duration because of limited battery performance and technical restrictions of the device technologies.[6,7] Alternative solutions for pacing over longer time frames have required wireless power transmission, which allowed only brief intermittent pacing of mice under anesthesia[7] or the use of exteriorized passive connects for tethered pacing in rats.[8,9] There is currently no available technology for long-term pacing in ambulatory mice.

Here, we describe a fully implantable, programmable, and battery-powered pacemaker for freely moving mice that is capable of continuous pacing over months. The device has been developed from a clinical-grade miniaturized pacemaker, which was modified with a custom epicardial lead and firmware for high-rate atrial or ventricular pacing. We present a surgical procedure and pacing parameters for robust operation over up to 4 weeks duration, and we use the device in 3 distinct applications. First, we use it in a model of ventricular pacing to treat high-grade heart block at the atrioventricular node. Recent work has demonstrated a critical role for macrophages in facilitating conduction at the atrioventricular node because macrophage depletion in the *Cd11b*^{DTR} mouse leads to heart block.[10] We demonstrate here the ability to pace macrophage-depleted mice with complete heart block, which will permit essential studies of conduction properties in the diseased and healing atrioventricular node. Next, we introduce a new model of cardiomyopathy and heart failure in the mouse utilizing overdrive ventricular pacing. We report that continuous tachypacing of the ventricular apex results in a reduction in LV function, biomarker evidence of heart failure, fibrosis, and an increase in the myeloid cell population in the myocardium. Finally, we establish chronic high-rate pacing of the atrium, which does not lead to reduced ventricular function but increases the inducibility of atrial fibrillation.

Methods

The data that support the findings of this study are available from the corresponding author on reasonable request.

Mice

All animal studies conformed to the National Institutes of Health Guide for the Care and Use of Laboratory Animals and were performed with the approval of the Subcommittee on Animal Research Care at Massachusetts General Hospital (2014N000078). C57BL/6 (stock 000664) and B6.FVB-Tg(ITGAM-DTR/EGFP)34Lan/J (*Cd11b*^{DTR}, stock 006000) were purchased from Jackson Laboratory. All experiments were performed with 8- to 70-week-old male and female animals and were carried out using age- and sex-matched groups. All animals were on a C57BL/6 background and were maintained in a pathogen-free environment of the Massachusetts General Hospital animal facility.

Macrophage depletion in *Cd11b*^{DTR} mice was achieved by a single intraperitoneal injection of diphtheria toxin (DT, 25 ng/g body weight).[10] C57BL/6 mice injected with DT were used as controls.

Surgical Procedures

Pacemaker Placement

Mice were given subcutaneous buprenorphine (0.05 mg/kg) for analgesia 30 to 60 minutes before procedures. Anesthesia was induced

with 3% isoflurane in 95% O_2. Each anesthetized mouse was shaved at the dorsal neck region and left side of the thorax using hair clippers, and then residual hair was removed with a depilatory cream (Nair) applied for 60 s. Excess cream was removed with gauze, and the sites were wiped with 70% isopropyl alcohol. The mouse was initially placed in prone position with anesthesia applied through a nose cone (1.5%–2% isoflurane in 95% O_2). Absence of toe pinch pain response was confirmed before starting surgery. A transverse skin incision ≈10 mm in length was made in the dorsal neck region using surgical scissors. The subcutaneous tissues were separated using blunt dissection, and a longitudinal pocket was made along the dorsum of the animal of ≈25 mm also using gentle blunt dissection with the scissors. The pacemaker was then advanced into the pocket with the lead facing caudally. A 5.0 nylon suture (Ethicon) was used to anchor the cranial aspect of the device to the subcutaneous fat in the dorsal region. The pacemaker lead was allowed to rest along the pulse generator in the pocket for later retrieval during the procedure. The dorsal neck incision was then closed using a 6.0 silk suture (Ethicon) in a continuous running stitch. Next, the animal was placed in supine position and intubated using a small animal laryngoscope and a 22G angiocath (Exel 22G Safelet Cath 0.90×25 mm) as an endotracheal tube. The angiocath was connected to a small animal ventilator (VentElite; Harvard Apparatus) set to provide volume control ventilation with tidal volume of 500 µL and respiratory rate of 120 breaths per minute. Satisfactory rise of the chest with ventilation was confirmed before proceeding with surgery. Anesthesia was maintained through the ventilator using 1.5% to 2% isoflurane in 95% O_2, with precise anesthesia dosing set to ensure negative toe pinch response. Subsequent surgical steps were performed with the aid of a dissecting stereo microscope. The animal was placed in right lateral decubitus position with the left arm raised in the cranial direction. A skin incision of ≈15 mm in length was next made from the tip of the xiphoid process extending toward the left axilla using surgical scissors. Low-temperature cautery was then used to cut through the subcutaneous fat and the superficial muscular layer to expose the ribs using caution not to injure the pectoralis muscle with its insertion running along the sternum. At this point, using a pair of fine forceps, the subcutaneous tissues were gently separated along a narrow tunnel back to the caudal end of the pacemaker device in the dorsal pocket. The pacemaker lead was located and then pulled through the tunnel into the field of view of the incision space. The lead was also tunneled through the caudal side of the superficial muscle layer, which had previously been separated. Next, the ribs were separated through a left thoracotomy in the intercostal space between the fourth and fifth ribs using blunt separation with the tips of the surgical scissors, which exposes the heart and lungs. The delicate parietal pericardium was then incised and gently separated using 2 pairs of fine surgical forceps. Then the pacemaker lead was tunneled through the fifth intercostal space and brought into proximity with the heart. Care is taken during tunneling of the lead to avoid excess tension or bend in the lead and to ensure that the tunnel pathway provides the most anatomically direct route between the pulse generator and the heart. The exposed wire tip of the pacemaker lead was secured to the heart using an 8.0 monofilament suture (Ethicon) passed as superficially as possible through the epicardial myocardium so as to avoid significant myocardial injury. With the lead secured, a 20G angiocath was passed through the superficial muscle layer and the fifth intercostal space into the left pleural cavity for use as a chest tube. The fourth and fifth ribs were then reapproximated and closed using 1 or 2 interrupted sutures with 6.0 silk suture. The superficial muscular layer was also closed with 6.0 silk suture. At this point, gentle suction was applied to the angiocath chest tube using a 1 mL syringe to remove remaining air in the closed chest cavity, and the chest tube was withdrawn from the body maintaining gentle suction. Retention sutures were now placed on the pacemaker lead, securing it directly to the superficial muscle layer in 2 locations. In some mice, an additional retention suture was placed tying the pacemaker lead to the fifth rib itself for greater stabilization. A small drop of cyanoacrylate glue was applied at the site of the lead passing through the superficial muscle layer to provide further anchoring support. Finally, the skin incision was closed using a running 6.0 silk suture. The pacemaker threshold was next tested using a Medtronic programmer and a surface ECG. At this point, the anesthesia was turned off, and the animal allowed to wake while continuing mechanical ventilation. When the mouse was sufficiently breathing on its own above the ventilator set rate, the endotracheal tube was removed, and the mouse was allowed to fully recover on a heating pad under observation. The surgical procedure for chronic pacing was optimized in 13 mice. Lead failure occurred after 1 week in several mice because of retraction of the lead from the superficial epicardial suture location. This was remedied by careful attention to the placement of the retention sutures and the use of cyanoacrylate glue to secure the lead along the chest wall to the superficial muscle layer.

Sham Surgery

The animal was given analgesia, anesthetized, shaved, and intubated as described above. Next, each animal underwent left thoracotomy as described above, and the pericardium was separated. The incision was then closed in standard fashion and the animal allowed to awaken, extubate, and recover under observation.

Pacemaker Interrogation

The implanted pacemaker was activated and controlled using a Medtronic programmer equipped with specialized software settings to allow direct memory programming of the mouse pacemaker with custom RAMware. The custom RAMware overrides the high-rate limit on

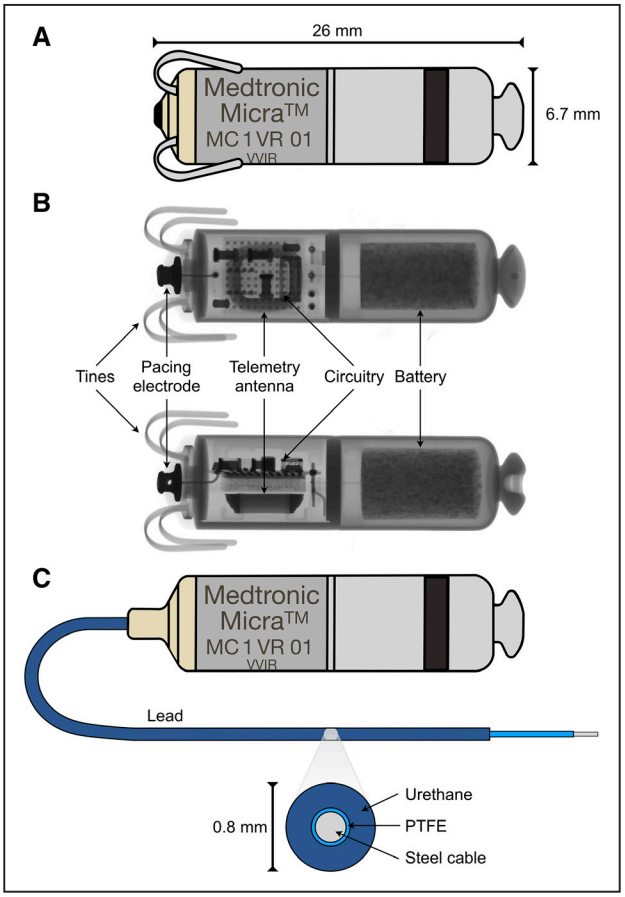

Figure 1. Adaptation of the clinical pacemaker to a fully implantable mouse pacemaker. A, Schematic diagram illustrating the clinical device for endocardial pacing. **B**, X-ray images of the pacemaker indicating the fixation tines, pacing electrode, telemetry antenna, circuitry, and battery. **C**, Schematic of the epicardial pacing device for use in mice. The tines were replaced with a 50 mm flexible pacing lead attached to a custom-made header machined from polyether ether ketone. The lead consists of a polytetrafluoroethylene (PTFE)-coated steel cable with an additional layer of urethane insulation. Fifteen millimeters of urethane and 5 mm of PTFE insulation are removed from the distal end of the lead to expose the steel cable, which is used as pacing electrode.

the commercial device enabling high-rate pacing. Communication with the device is achieved with radiofrequency telemetry allowing wireless programming using a standard telemetry head. Mice were generally anesthetized during interrogation to allow for simultaneous measurement of surface ECG. The pacing threshold was determined by varying the output voltage of the device and looking for the lowest possible value that achieved sustained capture of pacing on the surface ECG.

Please see the Detailed Methods section in the Online Data Supplement for surface ECG, echocardiography, electrophysiological study, computed tomography imaging, tissue processing, flow cytometry, quantitative polymerase chain reaction, histology, and statistics.

Results

Pacemaker Design and Surgical Procedure

An implantable device for chronic pacing experiments in ambulatory mice requires a small form factor, low weight, durable lead design, and extended battery life to enable continuous pacing. To overcome substantial design challenges and to provide a device that could be more readily available in other labs, we developed a specialized rodent version of the Micra pacemaker, which is currently the smallest clinical pacemaker in the world. The clinical device is a full-featured, rate-responsive miniature pacemaker that is used to pace the human heart after catheter-directed implantation into the trabeculae of the right ventricle. The device is 26 mm long and 6.7 mm in diameter (Figure 1A) with casing made from titanium and insulated with a parylene coating except for the titanium nitride ring electrode on the proximal end of the device. Figure 1B shows X-ray images of the pacemaker taken from orthogonal angles displaying the internal components. The device consists of an embedded circuit with onboard memory and telemetry capabilities via a radiofrequency antenna. The circuit interconnects to a battery and to 2 separate electrodes, one on the distal end of the device and the other to a ring electrode on the proximal end of the device body. We modified the device for use in mice as shown in Figure 1C: (1) The tines and pacing electrode are replaced by a 50 mm flexible lead attached to a custom-made header machined from polyether ether ketone. The lead consists of a polytetrafluoroethylene-coated steel cable with an additional layer of urethane insulation. Fifteen millimeters of urethane and 5 mm of polytetrafluoroethylene insulation are removed from the distal end of the lead to expose the metal cable, which is used as pacing electrode. The weights for the modified devices used in this study were 1.78±0.01 g (mean±SEM; n=6). (2) The firmware of the device was redesigned to overcome the clinical pacing rate limit of 170 bpm. By using research-level programmer access, the device now maintains a 1200 bpm rate with a 7.50 V output while the rate response feature is disabled.

We next developed a surgical procedure for pacemaker implantation (Figure 2A), which is described in full detail in the Methods section. Briefly, the mouse is anesthetized in an induction chamber with 3% isoflurane mixed with oxygen and subsequently maintained through a nose cone at 1.5% to 2% isoflurane in 95% O_2. In the prone position, a short midline dorsal incision is made to open a subcutaneous pocket for the pacemaker, and the device is pressed gently into the pocket secured by the surrounding connective tissue and tethered with a suture on the proximal end. The mouse is intubated and ventilated and placed in the supine position or slight right lateral decubitus position to allow a left lateral thoracotomy at the level of the

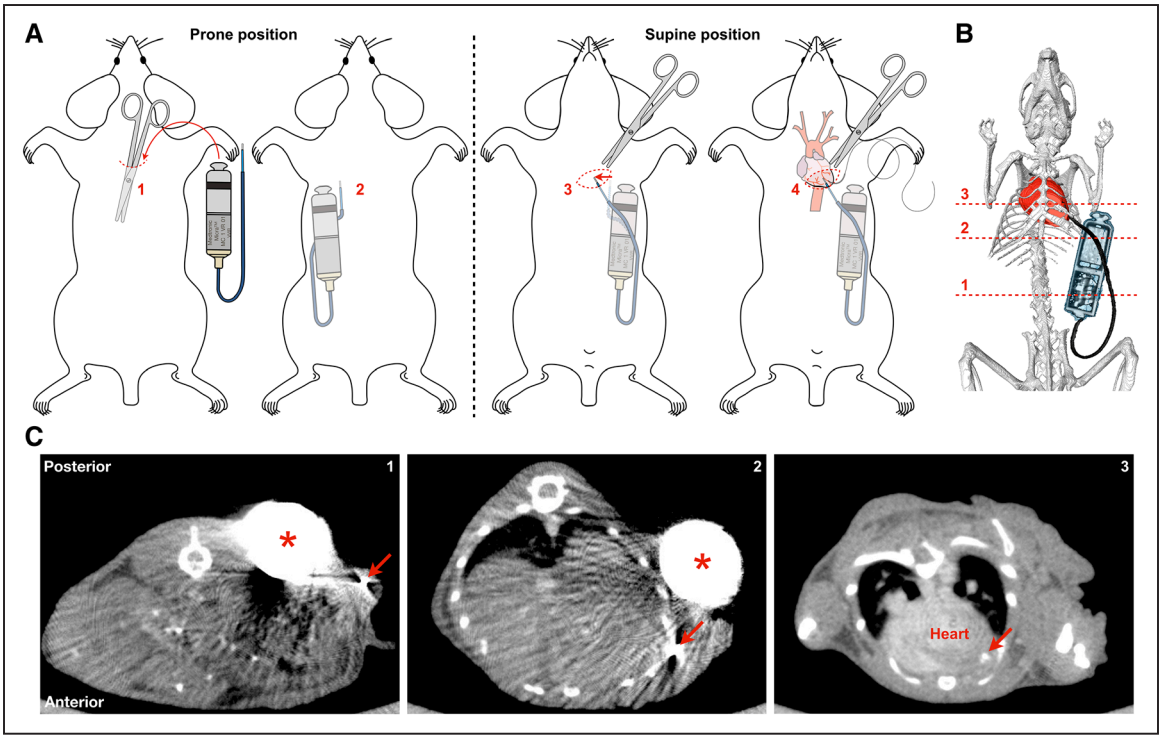

Figure 2. Overview of the surgical procedure for pacemaker implantation. A, (**Left**) Prone positioning of the mouse under anesthesia for insertion of the device in a subcutaneous pocket created by blunt dissection through a dorsal midline incision. (**Right**) Subsequent supine positioning for tunneling of the lead from the dorsal pocket through a left lateral thoracotomy incision for epicardial placement. The lead is attached directly to either the atrium or the ventricle using a superficial suture. **B**, Computed tomography (CT) of a mouse successfully implanted with a mouse pacemaker. **C**, Cross-sectional CT images are shown sequentially from the caudal to cranial direction (**left** to **right**). *the device; arrows indicate the lead.

fourth intercostal space, exposing the heart and left lung. The flexible pacemaker lead is tunneled using blunt dissection from the dorsal pocket via the subcutaneous space and through the lateral thoracotomy incision and secured to either the left atrial appendage for atrial pacing or to the ventricular apex near the insertion of the right ventricle for ventricular pacing using a superficial epicardial suture in a manner analogous to epicardial pacing leads placed after cardiac surgery in humans. After attachment of the epicardial electrode, the pacing threshold is determined by overdrive pacing of the heart. The surgical incisions are closed, and the mouse is allowed to recover with oxygen on a heating pad until extubation. To document the position of the device and the lead, we performed X-ray computed tomography after pacemaker implantation. Three-dimensional computed tomography reconstruction and cross-sectional computed tomography images (Figure 2B and 2C) illustrate the desired placement of the implant. Mice recovered well from surgery, and no postoperative deaths were observed.

In Vivo Testing of the Pacemaker

The mouse pacemaker is a single chamber pacemaker, but depending on the location of the electrode, it can provide atrial or

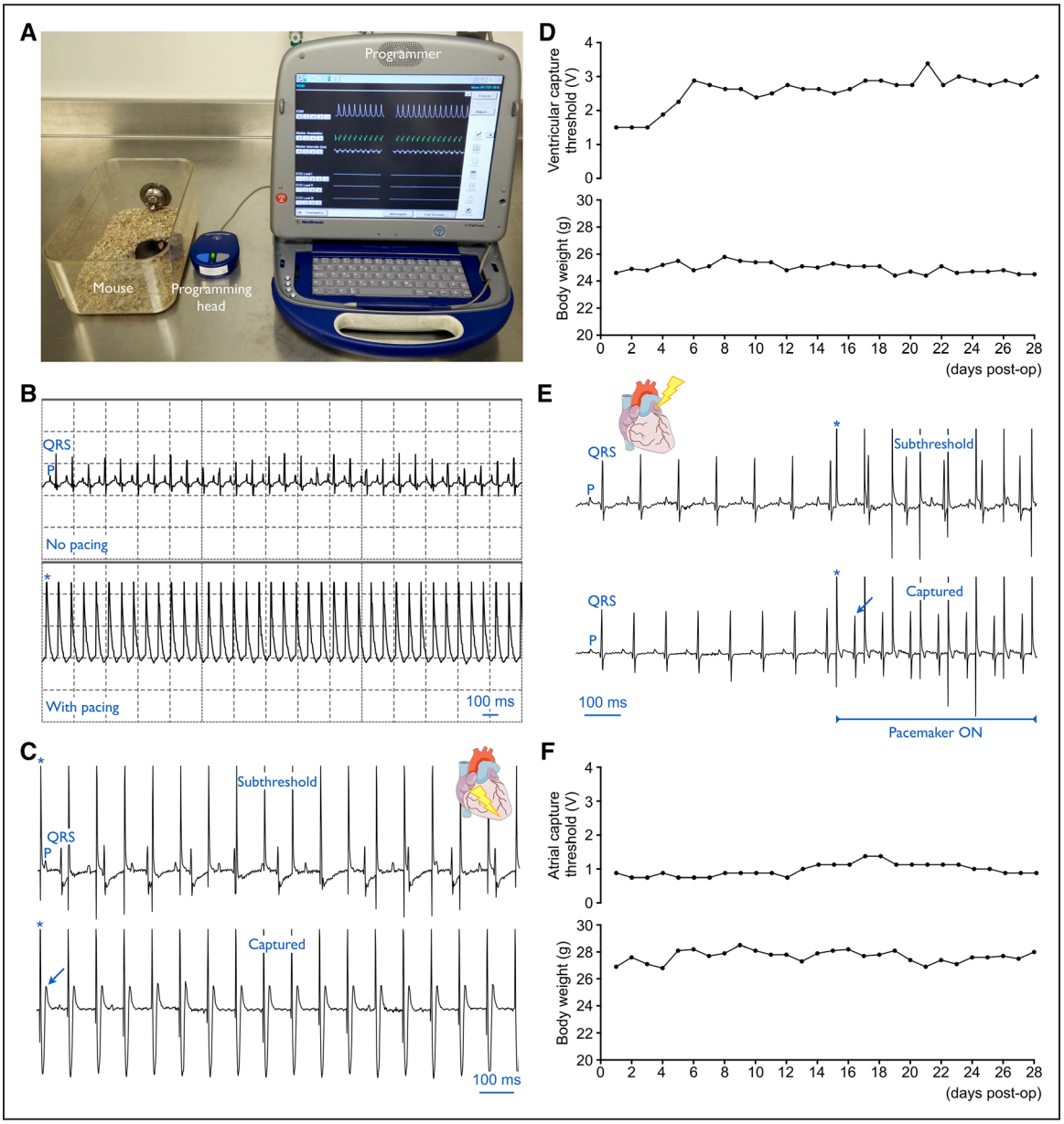

Figure 3. In vivo testing of the pacemaker for long-term pacing. A, Experimental setup to interrogate and program the implanted pacemaker. **B**, Representative electrogram tracings without pacing (**top**) and with overdrive ventricular pacing at 750 bpm (**bottom**). P and QRS indicate the intrinsic P wave and QRS complex, respectively; *pacing spike. **C**, Representative surface ECG tracings of a mouse stimulated at a subthreshold (**top**) or captured (**bottom**) amplitude. P and QRS indicate the intrinsic P wave and QRS complex, respectively; *pacing spikes; arrow indicates ventricular capture. **D**, Ventricular capture threshold (**top**) and body weight (**bottom**) over 4 wk for a representative mouse implanted with the mouse pacemaker. **E**, Representative surface ECG tracings from a mouse with the device implanted in an atrial pacing configuration. The lead is attached to the left atrial appendage. Tracings are shown before and after pacemaker activation at subthreshold (**top**) or captured (**bottom**) output amplitudes. P and QRS indicate the intrinsic P wave and QRS complex, respectively; *pacing spikes; arrow indicates the conducted QRS following atrial capture. **F**, Atrial capture threshold (**top**) and body weight (**bottom**) over 4 wk for a mouse implanted with the mouse pacemaker. Post-op indicates postoperative.

ventricular pacing. The device is programmed using a standard clinical programmer containing testing software that allows direct memory communication to program and download a custom high-rate pacing RAMware into the modified pacemaker (Figure 3A). Online Table I presents programmable settings used for implanted devices during our studies. Sensing mode is configured with maximal sensitivity, whereas in pacing mode, the output is set by testing the capture threshold and setting the amplitude 1.5–2× above the threshold. The rate can be programmed between 30 and 1200 bpm in the modified device. Cardiac electrograms during normal sinus rhythm and ventricular pacing at 750 bpm were recorded with the wireless programmer (Figure 3B). During every interrogation session, a surface ECG was taken to ensure proper function and to determine the pacing threshold (Figure 3C). Figure 3D displays the ventricular capture threshold and body weight of a representative mouse paced for 4 weeks at 750 bpm. The observed increase in the capture threshold over the first days after implantation corresponds with healing and mild fibrosis of the tissue in contact with the lead and is also seen after pacing lead implantation in humans. After implantation, mice were active, had normal eating and hygiene habits, and stable body weights (Figure 3D). Taken together, this indicates that mice tolerated the device well.

For atrial pacing, we implanted the lead in contact with the left atrial appendage (Figure 3E), which is the most readily accessed atrial structure from a left thoracotomy incision.

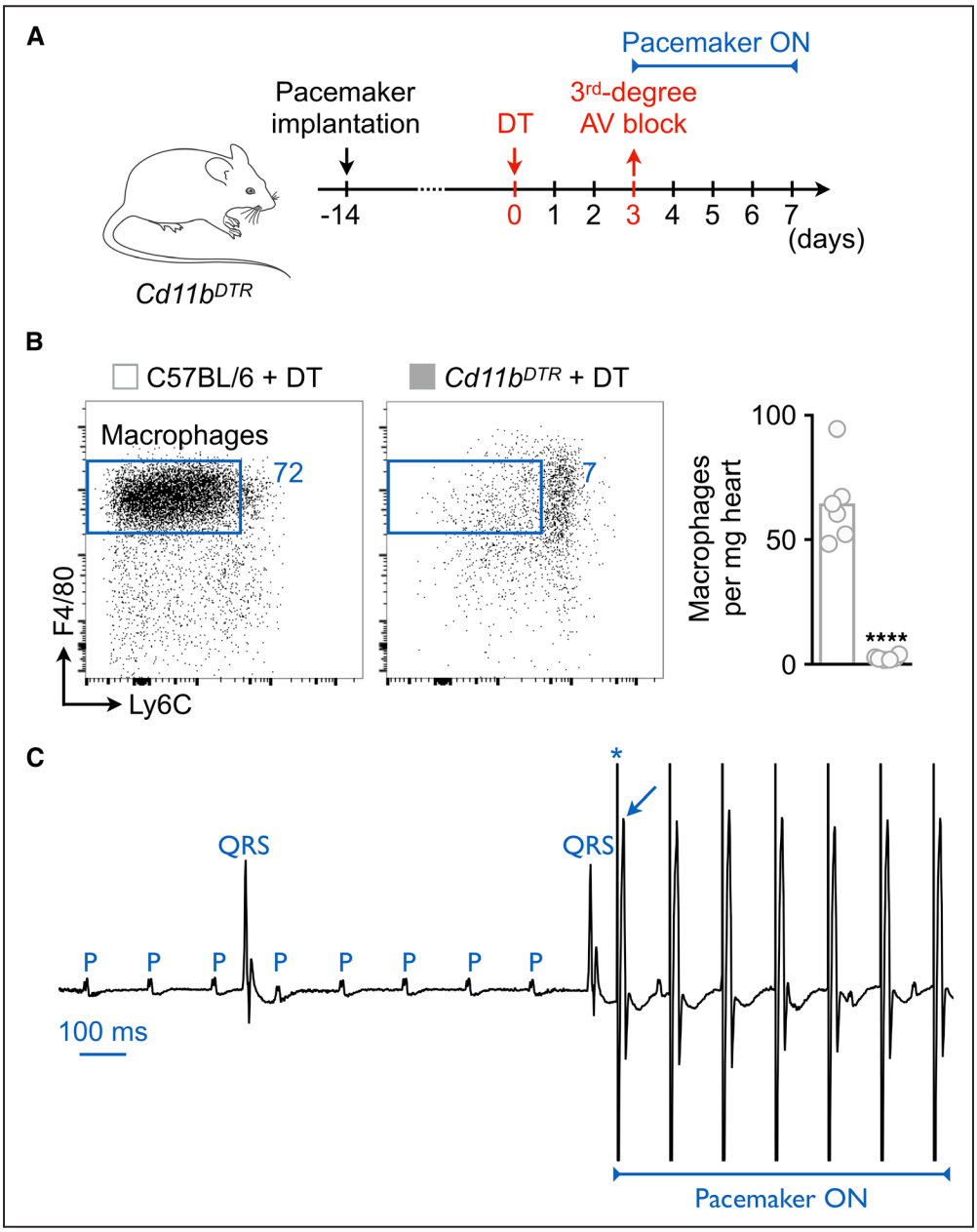

Figure 4. Pacemaker use in a mouse model of third-degree atrioventricular (AV) block. A, Experimental outline for macrophage depletion and induction of AV block. **B**, Flow cytometric quantification of cardiac macrophages 3 d after intraperitoneal injection of diphtheria toxin (DT) into C57BL/6 and *Cd11b*^{DTR} mice. Bars indicate means; n=6 mice per group; unpaired *t* test; ****P<0.0001. **C**, ECG of a macrophage-depleted *Cd11b*^{DTR} mouse 7 d post-DT with third-degree AV block before and after pacemaker activation. P and QRS indicate the intrinsic P wave and QRS complex before pacemaker activation. Each pacing spike (*) is followed by a QRS complex (arrow) demonstrating ventricular capture.

We determined the atrial capture threshold daily via surface ECG for a total of 4 weeks (Figure 3E). During the 4-week follow-up period, the capture threshold and the body weight remained stable (Figure 3F).

The estimated battery longevity of the device for human use is ≈10 years assuming a 1.5 V output, 600 Ω, 60 bpm, 100% pacing, and 0.24 ms nominal pulse width duration.[11] We used the mouse pacemaker for up to 165 pacing days at 550 to 1200 bpm, 100% pacing, and 0.24 ms pulse width duration without evidence of performance degradation (Online Table II).

Pacing in a Mouse Model of Complete Heart Block and Bradycardia

Atrioventricular node disease is common in humans and potentially lethal if it progresses to complete atrioventricular block and is not treated with a pacemaker.[2] Disorders of the

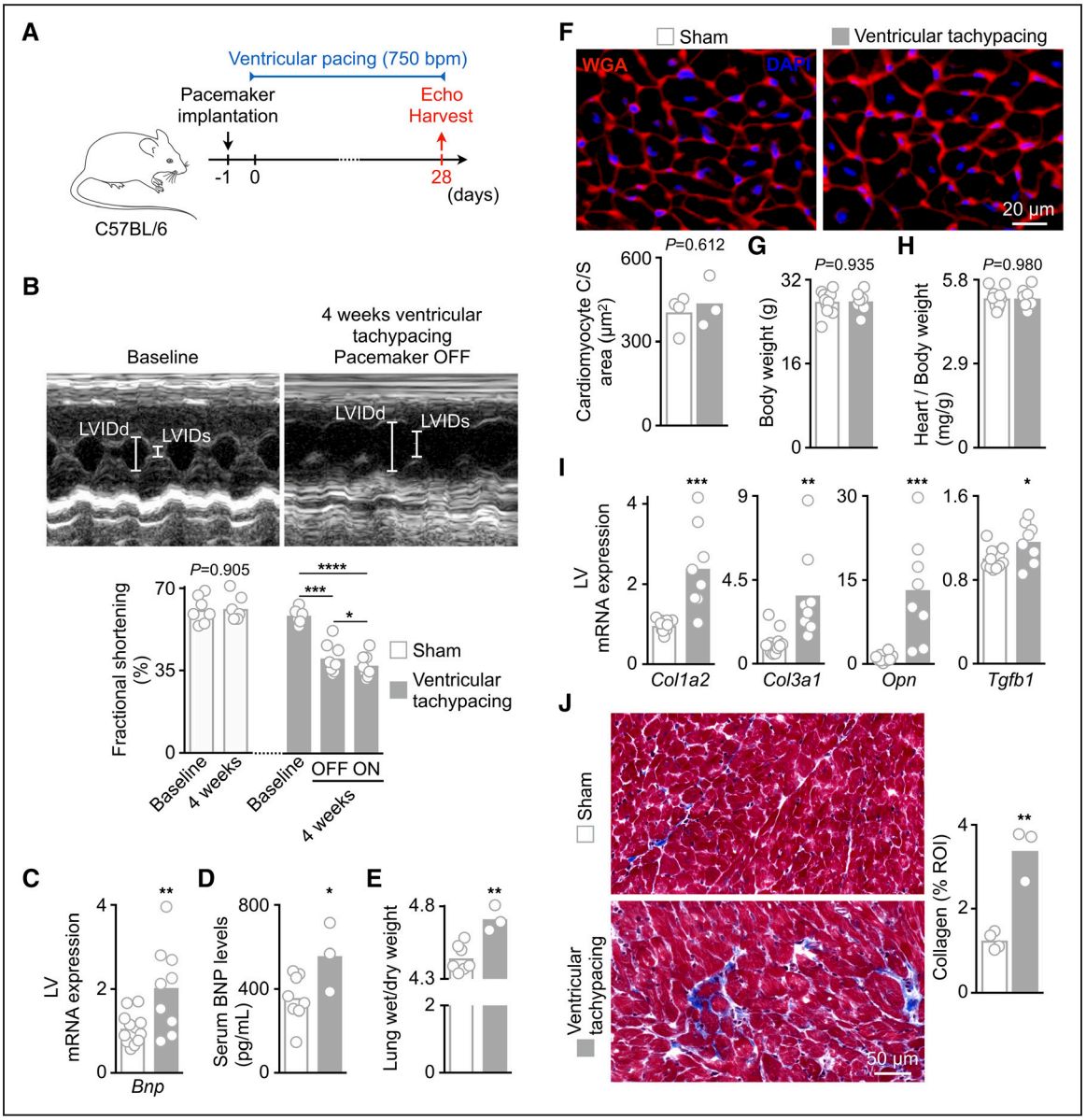

Figure 5. Ventricular tachypacing-induced model of cardiomyopathy. A, Experimental outline to generate ventricular tachypacing-induced cardiomyopathy by 4-wk overdrive apical pacing at 750 bpm. **B**, Functional evaluation of hearts undergoing ventricular pacing for 4 wk by echocardiography. (**Top**) Representative M-mode echocardiographic images acquired with the pacemaker turned off indicating left ventricular (LV) internal diameter at end diastole and end systole (LVIDd and LVIDs, respectively) before and after 4-wk overdrive ventricular pacing. (**Bottom**) LV fractional shortening in sham and ventricular tachypacing-induced cardiomyopathy mice with and without active pacing; paired *t* test and repeated measures 1-way ANOVA followed by Tukey test. **C**, Relative brain natriuretic peptide (*Bnp*) expression levels by quantitative polymerase chain reaction (qPCR) in LV from sham and ventricular tachypacing-induced cardiomyopathy mice. **D**, Serum BNP levels by ELISA in sham and ventricular tachypacing-induced cardiomyopathy mice. **E**, Lung wet-to-dry weight ratio in sham and ventricular tachypacing-induced cardiomyopathy mice. **F**, (**Top**) Representative immunofluorescence images of LV from sham and ventricular tachypacing-induced cardiomyopathy mice stained with WGA (wheat germ agglutinin; red) and DAPI (4′,6-diamidino-2-phenylindole; blue). (**Bottom**) Bar graph shows cardiomyocyte cross-sectional (C/S) area in sham and ventricular tachypacing-induced cardiomyopathy mice. **G** and **H**, Body weight (**G**) and heart-to-body weight ratio (**H**) in sham and tachypacing-induced cardiomyopathy mice. **I**, Relative expression levels of fibrosis-related genes by qPCR in LV from sham and tachypacing-induced cardiomyopathy mice. **J**, (**Left**) Representative Masson's trichrome stain of LV from sham and tachypacing-induced cardiomyopathy mice. (**Right**) Percentage of positive collagen staining per region of interest (ROI). Bars indicate means; n=3 to 12 mice per group; unpaired *t* test unless stated differently; **P*<0.05, ***P*<0.01, ****P*<0.001, and *****P*<0.0001.

atrioventricular node are generally progressive over time and, therefore, difficult to model in the mouse without availability of chronic pacing technologies. We recently discovered that macrophage ablation in *Cd11b*^{DTR} mice induces progressive heart block. In this transgenic mouse, the human DT receptor is expressed in myeloid cells, and injection of low DT doses depletes CD11b^{+} cells, including cardiac resident macrophages in the atrioventricular node.[10,12] We previously observed rapid onset of atrioventricular block in 88% of DT-injected *Cd11b*^{DTR} mice at a dose of 25 ng/g body weight.[10] The model of atrioventricular block in mice may have interesting applications in the study of conduction disease, especially if mice can be rescued with pacing. To enable pacing of mice with atrioventricular conduction failure, we programmed the device to serve as a backup pacemaker for *Cd11b*^{DTR} mice progressing to third-degree atrioventricular block. Pacemakers were implanted 14 days before macrophage depletion. The pacemaker was switched on when mice went into complete heart block (Figure 4A; n=4). Maximum depletion of cardiac macrophages occurred 3 days after DT injection (Figure 4B), which coincided with the time of third-degree atrioventricular block onset.[10] Mice with complete heart block exhibited an atrial rate of 445±47 bpm with a slower ventricular escape rate of 313±59 bpm (mean±SEM; n=4; paired *t* test; $P<0.05$). Ventricular pacing restored a physiological heart rate of 550 bpm at a mean threshold of 2.25±0.57 V (mean±SEM; n=4). Figure 4C provides a representative ECG of a *Cd11b*^{DTR} mouse 7 days after macrophage ablation with complete heart block before and after pacemaker activation.

Ventricular Pacing-Induced Cardiomyopathy

We next developed a murine model of chronic pacing-induced cardiomyopathy (Figure 5A). Healthy mice with normal baseline cardiac function measured by echocardiography (Figure 5B) were implanted with pacemakers with the lead secured to the ventricular apex near the insertion of the right ventricle at the septum. These mice were overdrive paced at 750 bpm for 4 weeks with a mean threshold of 2.28±0.07 V (mean±SEM; n=8), after which LV function was again measured and the hearts harvested for analysis. Overdrive pacing significantly reduced fractional shortening after 4 weeks with and without active pacing, demonstrating a reduction in LV function even when the pacemaker is switched off and native conduction is restored (Figure 5B). The LV internal diameter at end diastole, an index for LV dilation, was not altered (Online Table III), whereas cardiac expression of brain natriuretic peptide (*Bnp*), serum BNP levels and lung wet-to-dry weight ratio were increased (Figure 5C–5E). Chronic tachypacing did not change cardiomyocyte size, body weight, and heart-to-body weight ratio compared with sham controls (Figure 5F–5H). Cardiac expression of fibrotic markers, specifically collagen (collagen type I alpha 2 [*Col1a2*] and collagen type III alpha 1 [*Col3a1*]), osteopontin (*Opn*), and transforming growth factor beta 1 (*Tgfb1*), were significantly increased after 4-week overdrive pacing (Figure 5I), which corresponds with interstitial fibrosis of the LV myocardium (Figure 5J). These findings suggest development of LV dysfunction without profound cardiac dilation or hypertrophy, but with evidence of extracellular matrix remodeling.

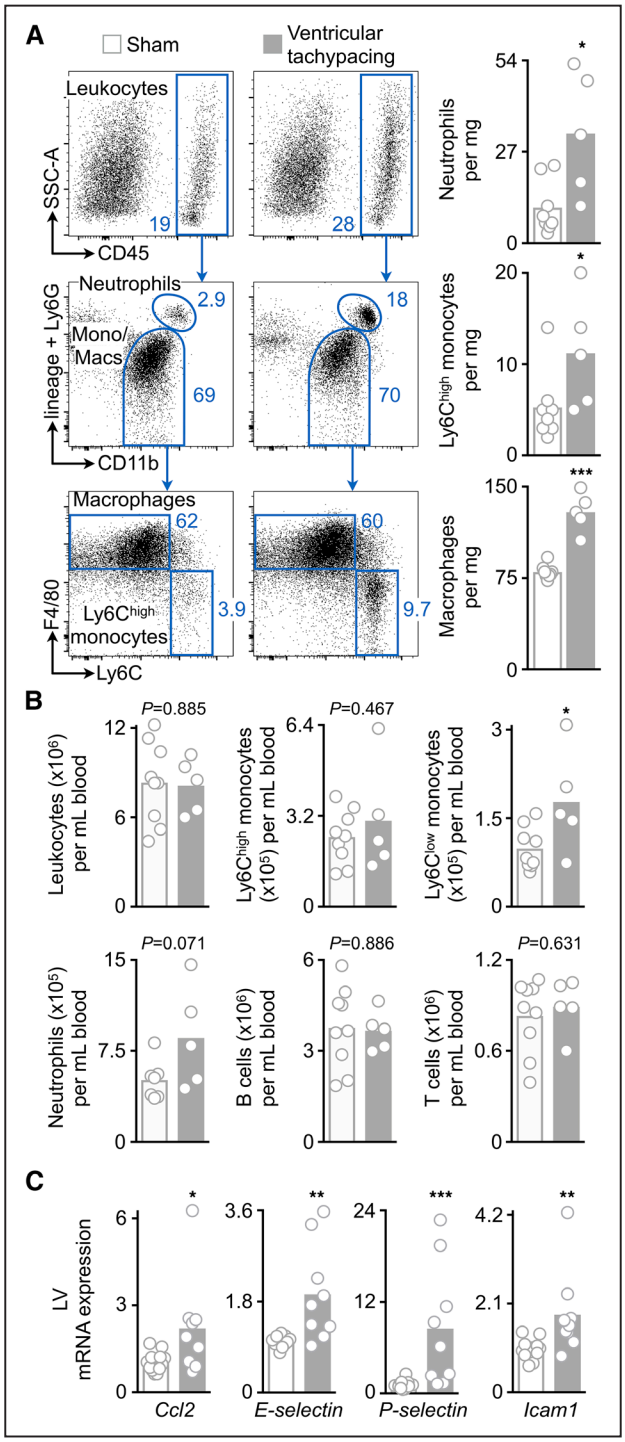

Figure 6. Cardiac inflammation in ventricular tachypacing-induced cardiomyopathy. A, Flow cytometric quantification of myeloid cell populations in hearts from sham and tachypacing-induced cardiomyopathy mice. (**Left**) Representative flow cytometry plots; (**right**) number of cell populations per mg of heart tissue; Mann-Whitney test. **B**, Flow cytometric quantification of myeloid cells and lymphocytes in blood from sham and tachypacing-induced cardiomyopathy mice. **C**, Relative expression levels of different chemokines and adhesion molecules by quantitative polymerase chain reaction in left ventricle (LV) from sham and tachypacing-induced cardiomyopathy mice; Mann-Whitney test. Bars indicate means; n=5 to 12 mice per group; unpaired *t* test unless stated differently; **P*<0.05, ***P*<0.01, and ****P*<0.001. Mono/Macs indicates monocytes/macrophages; and SSC-A, side scatter area.

Recent work indicates the involvement of the innate immune system, and specifically cardiac macrophages, in chronic heart failure.[13–17] We found that the number of cardiac neutrophils, Ly6C^{high} monocytes and macrophages rose in the hearts of mice with tachypacing-induced cardiomyopathy (Figure 6A). Interestingly, only circulating Ly6C^{low} monocyte levels significantly increased after 4-week overdrive pacing (Figure 6B). To determine whether accumulation of myocardial macrophages relies on recruitment of monocytes from the blood in this setting, we measured expression of chemokines and adhesion molecules in myocardial tissue from sham and tachypacing-induced cardiomyopathy mice (Figure 6C). The increased chemokine and adhesion molecule expression suggests a contribution of monocyte recruitment to cardiac macrophage expansion.

Chronic Atrial Tachypacing

Chronic atrial tachypacing has been used in large animals to generate atrial fibrillation,[18] but this technique has been unavailable for mice because of the lack of miniaturized pacemakers for long-term implantation in the mouse. We sought to evaluate the capability for chronic, high-rate atrial pacing in the mouse by implanting our device in atrial configuration and pacing for 4 weeks at 1200 bpm (Figure 7A). The implantation was well tolerated by all mice (n=7) and resulted in reliable atrial capture with mean threshold of 0.93±0.02 V (mean±SEM; n=7) and 2:1 ventricular conduction seen on surface ECG under anesthesia (Figure 7B), resulting in a ventricular rate of 600 bpm. Mice were interrogated daily for 4 weeks. We did not observe spontaneous atrial fibrillation in awake (Figure 7C) or anesthetized animals (Figure 7D). We then performed an in vivo electrophysiological study after 4-week atrial tachypacing to further investigate the electrophysiological properties of the atria. The atrial effective refractory period measured at 100 ms cycle length was similar in both sham-operated controls and atrial paced mice (Figure 7E). Whereas only 1 out of 7 sham mice showed inducible atrial fibrillation, 4 out of 7 atrial paced mice were more prone to atrial fibrillation (Figure 7E; χ^2 test; P=0.094). Interestingly, the sinus node recovery time at 80 ms cycle length was reduced after 4-week overdrive pacing (Online Table IV). We did not observe differences in the atrioventricular node function or ventricular effective refractory period (Online Table IV). There was no change in fractional shortening (Figure 7F), LV diameter (Online Table III) and cardiac *Bnp* levels (Figure 7G) after 4 weeks of high-rate atrial pacing.

Because our data indicate that atrial tachypacing may predispose the atria to fibrillation but preserves LV function,

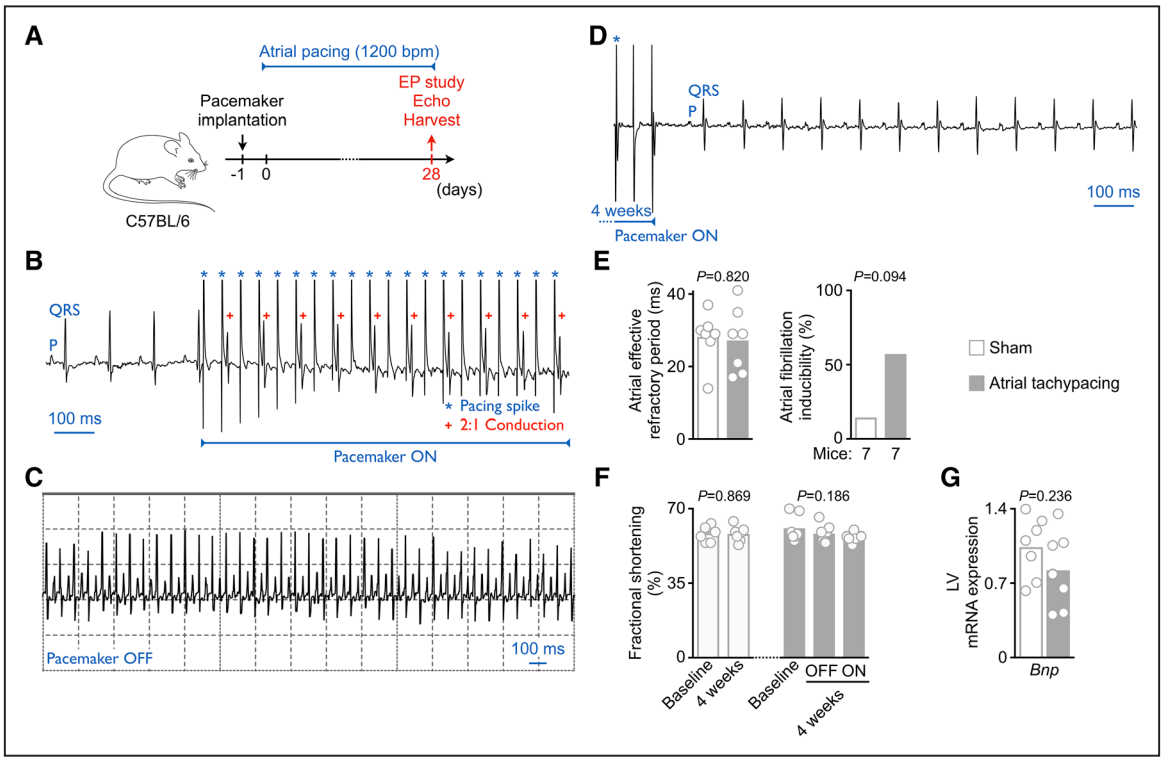

Figure 7. Chronic atrial tachypacing using the mouse pacemaker. A, Experimental outline to investigate atrial tachypacing by 4-wk overdrive atrial pacing at 1200 bpm. **B**, Representative surface ECG tracing from a mouse with the device implanted in an atrial pacing configuration before and after pacemaker activation at 1200 bpm. P and QRS indicate the intrinsic P wave and QRS complex, respectively; *pacing spikes; plus signs indicate the conducted QRS following atrial capture (2:1 conduction). **C**, Representative electrogram tracing of an awake mouse after 4-wk overdrive atrial pacing at 1200 bpm. The tracing was recorded immediately after pacemaker inactivation and shows normal sinus rhythm. **D**, Representative surface ECG tracing from an anesthetized mouse after 4-wk overdrive atrial pacing at 1200 bpm. The tracing was recorded immediately after pacemaker inactivation and shows normal sinus rhythm. *pacing spike; P and QRS indicate the intrinsic P wave and QRS complex, respectively. **E**, Functional evaluation of the electrophysiological (EP) properties of the atria in mice undergoing atrial tachypacing for 4 wk by EP study. (**Left**) Atrial effective refractory period at 100 ms pacing frequency and (**right**) atrial fibrillation inducibility in sham-operated and atrial paced mice (χ^2 test). **F**, Left ventricular (LV) fractional shortening by echocardiography in sham-operated and atrial paced mice with and without active pacing; paired *t* test and repeated measures 1-way ANOVA followed by Tukey test. **G**, Relative brain natriuretic peptide (*Bnp*) expression levels by quantitative polymerase chain reaction in LV from sham-operated and atrial paced mice. Bars indicate means; n=7 mice per group; unpaired *t* test unless stated differently.

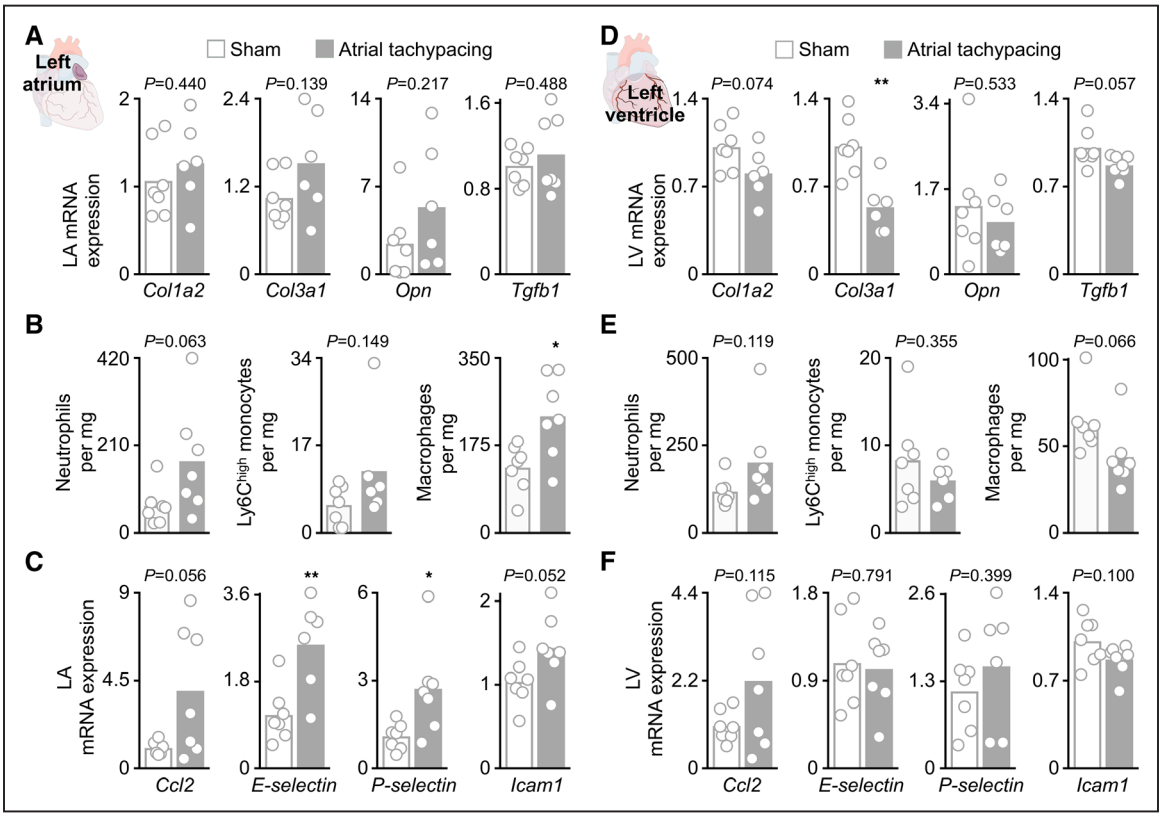

Figure 8. Fibrotic and inflammatory response in atrial and ventricular tissues after chronic atrial tachypacing. A, Relative expression levels of fibrosis-related genes by quantitative polymerase chain reaction (qPCR) in left atrium (LA) from sham-operated and atrial paced mice. **B**, Flow cytometric quantification of myeloid cell populations in LA from sham-operated and atrial paced mice. **C**, Relative expression levels of different chemokines and adhesion molecules by qPCR in LA from sham-operated and atrial paced mice. **D**, Relative expression levels of fibrosis-related genes by qPCR in left ventricle (LV) from sham-operated and atrial paced mice. **E**, Flow cytometric quantification of myeloid cell populations in LV from sham-operated and atrial paced mice. **F**, Relative expression levels of different chemokines and adhesion molecules by qPCR in LV from sham-operated and atrial paced mice. Bars indicate means; n=6 to 7 mice per group; unpaired *t* test; **P*<0.05 and ***P*<0.01.

we next compared the fibrotic and inflammatory response in both chambers. There was no change in the expression of fibrotic markers in the left atrium (Figure 8A), although the macrophage density rose after 4 weeks of high-rate atrial pacing (Figure 8B). The increased expression of *E-selectin* and *P-selectin* in chronically paced mice (Figure 8C) suggests a contribution of monocyte recruitment to left atrial macrophage expansion. In contrast, the left ventricle of mice undergoing atrial tachypacing for 4 weeks showed decreased *Col3a1* expression (Figure 8D), unaltered levels of innate immune cells (Figure 8E), and unchanged expression levels of chemokines and adhesion molecules (Figure 8F).

Discussion

Development of implantable pacing devices for mice has been long recognized as essential for fundamental research of conduction system disorders and heart failure, as well as investigation of the adverse effects from chronic pacing.[3] The clinical significance of open questions on aberrant conduction has driven several prior attempts to engineer devices appropriate for mice, but none to date has been capable of long-term continuous pacing for more than several days. Previously, key pitfalls have been the lack of sufficient battery life and high surgical implant mortality. Here, we have taken advantage of a recently introduced clinical-grade miniaturized pacemaker to develop a new implant for mice that is well tolerated, programmable, and capable of continuous epicardial pacing over weeks to months. Furthermore, we have optimized a surgical procedure to ensure reliable functioning of the implant for reproducible long-term studies. These advances provide access to long-term pacing in mice, a tool that was previously not available even in laboratories with substantial engineering expertise. We demonstrate ventricular pacing for up to 4 weeks duration, though the devices at this time were fully functioning and would have supported longer studies. Cumulatively over the course of this study, the devices were implanted in multiple mice and provided pacing for >5.5 months each without evidence of performance degradation. This demonstrates a sufficient battery life and stable lead performance. An epicardial lead configuration allowed ease of implantation and flexible configuration of the pacing site. We demonstrated both atrial and ventricular pacing with pacing thresholds that are stable over time. The dorsal implantation of the pulse generator is well tolerated by mice and does not affect their ambulation or activity levels. Wireless communication with the device enables not only testing of device functionality and battery life but also implantable telemetry functionality when the pacing mode is switched off.

The device allows previously impossible studies to be performed in mice. We demonstrate its first use for the

treatment of complete heart block and bradycardia in a model of atrioventricular block after macrophage depletion. This configuration will permit detailed survival studies and immunologic investigation of hypothetical atrioventricular nodal recovery after repopulation of tissue-resident macrophages. Elucidating the roles of macrophages and other cell types, such as conducting cardiomyocytes and fibroblasts, during atrioventricular node recovery will require long-term studies using pacing to support the animals during periods of bradycardia. More generally, complete atrioventricular block in humans leads to structural and electrical remodeling with risk for sudden cardiac death and heart failure. Atrioventricular block has been studied in larger animal models, including dogs, rabbits, and more recently in mice using radiofrequency atrioventricular node ablation.[19–21] Mice with complete atrioventricular block exhibit extreme bradycardia and frequent polymorphic ventricular tachycardia from acquired lengthening of repolarization time (QT interval) with high mortality.[21] Further investigations of atrioventricular node recovery and the physiology of atrioventricular block in mouse models, therefore, rely on the capability for ventricular pacing to prevent short-term mortality.

We have also used the pacemaker to create a chronic mouse model of tachypacing-induced cardiomyopathy. Rapid overdrive ventricular pacing for 4 weeks leads to a decline in LV function and biomarker evidence of congestive heart failure. Prior work has demonstrated that short-term overdrive right ventricular pacing leads to dyssynchrony, with septal wall contraction preceding the lateral wall contraction because of direct ventricular activation, and altered gene expression in the myocardium.[6] However, it has previously not been possible to evaluate the impact of long-term pacing and dyssynchrony on cardiac function, gene expression, and remodeling. In our study, 4 weeks of pacing triggered extracellular matrix changes evidenced by an increase in *Col1a2* and *Col3a1* gene expression, an increase in the expression of the profibrotic cytokine *Opn*,[22] and increased levels of *Tgfb1* expression which has pleiotropic effects on fibroblast differentiation and activation,[23] and interstitial fibrosis in the chronically paced hearts. These findings are accompanied by an increase in leukocytes in the myocardium, including neutrophils, Ly6C^{high} monocytes, and macrophages. Increased cell recruitment was likely triggered by upregulation of the chemokine (C-C motif) ligand 2 (*Ccl2*) and the endothelial cell adhesion molecules *E-selectin*, *P-selectin*, and intercellular adhesion molecule 1 (*Icam1*). Together, this suggests that pacing-induced cardiomyopathy associates with a state of myocardial inflammation, endothelial activation, and extracellular matrix remodeling. Notably, we did not observe ventricular dilation after 4 weeks of ventricular pacing which is seen in larger animal models with pacing-induced cardiomyopathy.[24] We speculate that our mouse data reflect the earlier stages of pacing-induced cardiomyopathy, which may result from a combination of constitutive overdrive pacing, as well as ventricular dyssynchrony from direct ventricular activation.

Atrial fibrillation, which contributes to heart failure and creates risk for stroke in patients, remains difficult to model in mice. Previous work indicated that rapid pacing of the atrium in mice can lead to atrial fibrillation.[25] We, therefore, evaluated the device functionality for high-rate atrial pacing. Four weeks of atrial tachypacing did not lead to spontaneous atrial fibrillation but may predispose to inducible atrial fibrillation, while LV function was preserved. Our finding of increased atrial macrophage numbers after atrial tachypacing aligns with prior work highlighting the association between inflammation and development of atrial fibrillation.[26] Future optimization of atrial tachypacing and its use in transgenic mice predisposed to developing atrial fibrillation[27–30] may prove critical to generating a reliable model of sustained atrial fibrillation for evaluation of novel pharmacotherapies in mice.

The ability to perform long-term pacing in the mouse will also enable many other important studies. It has not to date been possible to evaluate the impact of pacing-induced transient asynchrony in mouse models of heart failure without a chronic, programmable pacemaker. This recently proposed approach to treat heart failure with normal synchronous conduction promises to extend benefits of cardiac resynchronization therapy to many new patients,[31] but requires substantial further investigation to decipher the underlying mechanisms and to optimize the therapy. The embedded memory and processor on the device should also enable more complex electrophysiological stimulation protocols and custom pacing routines. Finally, although designed for use in mice, the device should be useful for similar applications in larger animals, such as rats or rabbits, where a small form factor, implantable, high-rate pacemaker may be required. Extrapolating further, the lead-modified device could also find use in humans, especially in pediatric patients where rapid growth leads to challenges with conventional endocardial lead implants.

Acknowledgments

We thank Greg Wojtkiewicz for assistance with imaging.

Source of Funding

This work was funded in part by federal funds from the National Institutes of Health (NIH) HL122208, HL139598, HL125428, and HL131495. M. Hulsmans was supported by a Massachusetts General Hospital Executive Committee on Research Tosteson and Fund for Medical Discovery Fellowship (2017A052660). A.D. Aguirre was supported by the American Heart Association (14FTF20380185) and by the Massachusetts General Hospital Physician Scientist Development Award. S. Cremer was supported by the Deutsche Forschungsgemeinschaft (CR 603/1-1). K.R. King was supported by NIH HL129168 and the American Heart Association (17IRG33410543). D.J. Milan was supported by NIH HL132905. M. Nahrendorf and F.K. Swirski were supported by the Massachusetts General Hospital Research Scholar Program.

Disclosures

M.D. Bonner is an employee of Medtronic PLC and an inventor on Micra-related patents. The other authors report no conflicts.

References

1. Epstein AE, DiMarco JP, Ellenbogen KA, et al; American College of Cardiology/American Heart Association Task Force on Practice Guidelines (Writing Committee to Revise the ACC/AHA/NASPE 2002 Guideline Update for Implantation of Cardiac Pacemakers and Antiarrhythmia Devices); American Association for Thoracic Surgery; Society of Thoracic Surgeons. ACC/AHA/HRS 2008 guidelines for device-based therapy of cardiac rhythm abnormalities: a report of the American College of Cardiology/American Heart Association Task Force on Practice Guidelines (Writing Committee to Revise the

ACC/AHA/NASPE 2002 guideline update for implantation of cardiac pacemakers and antiarrhythmia devices): developed in collaboration with the American Association for Thoracic Surgery and Society of Thoracic Surgeons. *Circulation*. 2008;117:e350–e408. doi: 10.1161/CIRCUALTIONAHA.108.189742

2. Brignole M, Auricchio A, Baron-Esquivias G, et al; ESC Committee for Practice Guidelines (CPG); Document Reviewers. 2013 ESC guidelines on cardiac pacing and cardiac resynchronization therapy: the Task Force on cardiac pacing and resynchronization therapy of the European Society of Cardiology (ESC). Developed in collaboration with the European Heart Rhythm Association (EHRA). *Eur Heart J*. 2013;34:2281–2329. doi: 10.1093/eurheartj/eht150
3. Kirk JA, Kass DA. Cellular and molecular aspects of dyssynchrony and resynchronization. *Heart Fail Clin*. 2017;13:29–41. doi: 10.1016/j.hfc.2016.07.003
4. Milan DJ, MacRae CA. Animal models for arrhythmias. *Cardiovasc Res*. 2005;67:426–437. doi: 10.1016/j.cardiores.2005.06.012
5. Nishida K, Michael G, Dobrev D, Nattel S. Animal models for atrial fibrillation: clinical insights and scientific opportunities. *Europace*. 2010;12:160–172. doi: 10.1093/europace/eup328
6. Bilchick KC, Saha SK, Mikolajczyk E, Cope L, Ferguson WJ, Yu W, Girouard S, Kass DA. Differential regional gene expression from cardiac dyssynchrony induced by chronic right ventricular free wall pacing in the mouse. *Physiol Genomics*. 2006;26:109–115. doi: 10.1152/physiolgenomics.00281.2005
7. Laughner JI, Marrus SB, Zellmer ER, Weinheimer CJ, MacEwan MR, Cui SX, Nerbonne JM, Efimov IR. A fully implantable pacemaker for the mouse: from battery to wireless power. *PLoS One*. 2013;8:e76291. doi: 10.1371/journal.pone.0076291
8. Mor M, Mulla W, Elyagon S, Gabay H, Dror S, Etzion Y, Liel-Cohen N. Speckle-tracking echocardiography elucidates the effect of pacing site on left ventricular synchronization in the normal and infarcted rat myocardium. *PLoS One*. 2014;9:e99191. doi: 10.1371/journal.pone.0099191
9. Mulla W, Etzion S, Elyagon S, Gillis R, Murninkas M, Konstantino Y, Mannhardt I, Eschenhagen T, Liel-Cohen N, Etzion Y. Prominent differences in left ventricular performance and myocardial properties between right ventricular and left ventricular-based pacing modes in rats. *Sci Rep*. 2017;7:5931. doi: 10.1038/s41598-017-06197-w
10. Hulsmans M, Clauss S, Xiao L, et al. Macrophages facilitate electrical conduction in the heart. *Cell*. 2017;169:510.e20–522.e20. doi: 10.1016/j.cell.2017.03.050
11. Ritter P, Duray GZ, Zhang S, Narasimhan C, Soejima K, Omar R, Laager V, Stromberg K, Williams E, Reynolds D; Micra Transcatheter Pacing Study Group. The rationale and design of the Micra Transcatheter Pacing Study: safety and efficacy of a novel miniaturized pacemaker. *Europace*. 2015;17:807–813. doi: 10.1093/europace/euv026
12. Duffield JS, Forbes SJ, Constandinou CM, Clay S, Partolina M, Vuthoori S, Wu S, Lang R, Iredale JP. Selective depletion of macrophages reveals distinct, opposing roles during liver injury and repair. *J Clin Invest*. 2005;115:56–65. doi: 10.1172/JCI22675
13. Lavine KJ, Epelman S, Uchida K, Weber KJ, Nichols CG, Schilling JD, Ornitz DM, Randolph GJ, Mann DL. Distinct macrophage lineages contribute to disparate patterns of cardiac recovery and remodeling in the neonatal and adult heart. *Proc Natl Acad Sci USA*. 2014;111:16029–16034. doi: 10.1073/pnas.1406508111
14. Sager HB, Hulsmans M, Lavine KJ, et al. Proliferation and recruitment contribute to myocardial macrophage expansion in chronic heart failure. *Circ Res*. 2016;119:853–864. doi: 10.1161/CIRCRESAHA.116.309001
15. King KR, Aguirre AD, Ye YX, et al. IRF3 and type I interferons fuel a fatal response to myocardial infarction. *Nat Med*. 2017;23:1481–1487. doi: 10.1038/nm.4428
16. Hulsmans M, Sager HB, Roh JD, et al. Cardiac macrophages promote diastolic dysfunction. *J Exp Med*. 2018;215:423–440. doi: 10.1084/jem.20171274
17. Liao X, Shen Y, Zhang R, et al. Distinct roles of resident and nonresident macrophages in nonischemic cardiomyopathy. *Proc Natl Acad Sci USA*. 2018;115:E4661–E4669. doi: 10.1073/pnas.1720065115
18. Yu J, Li W, Li Y, Zhao J, Wang L, Dong D, Pan Z, Yang B. Activation of β(3)-adrenoceptor promotes rapid pacing-induced atrial electrical remodeling in rabbits. *Cell Physiol Biochem*. 2011;28:87–96. doi: 10.1159/000331717
19. Tsuji Y, Opthof T, Yasui K, Inden Y, Takemura H, Niwa N, Lu Z, Lee JK, Honjo H, Kamiya K, Kodama I. Ionic mechanisms of acquired QT prolongation and torsades de pointes in rabbits with chronic complete atrioventricular block. *Circulation*. 2002;106:2012–2018.
20. Oros A, Beekman JD, Vos MA. The canine model with chronic, complete atrio-ventricular block. *Pharmacol Ther*. 2008;119:168–178. doi: 10.1016/j.pharmthera.2008.03.006
21. Bignolais O, Quang KL, Naud P, El Harchi A, Briec F, Piron J, Bourge A, Leoni AL, Charpentier F, Demolombe S. Early ion-channel remodeling and arrhythmias precede hypertrophy in a mouse model of complete atrioventricular block. *J Mol Cell Cardiol*. 2011;51:713–721. doi: 10.1016/j.yjmcc.2011.07.008
22. Lenga Y, Koh A, Perera AS, McCulloch CA, Sodek J, Zohar R. Osteopontin expression is required for myofibroblast differentiation. *Circ Res*. 2008;102:319–327. doi: 10.1161/CIRCRESAHA.107.160408
23. Dobaczewski M, Chen W, Frangogiannis NG. Transforming growth factor (TGF)-β signaling in cardiac remodeling. *J Mol Cell Cardiol*. 2011;51:600–606. doi: 10.1016/j.yjmcc.2010.10.033
24. Dixon JA, Spinale FG. Large animal models of heart failure: a critical link in the translation of basic science to clinical practice. *Circ Heart Fail*. 2009;2:262–271. doi: 10.1161/CIRCHEARTFAILURE.108.814459
25. Wakimoto H, Maguire CT, Kovoor P, Hammer PE, Gehrmann J, Triedman JK, Berul CI. Induction of atrial tachycardia and fibrillation in the mouse heart. *Cardiovasc Res*. 2001;50:463–473.
26. Hu YF, Chen YJ, Lin YJ, Chen SA. Inflammation and the pathogenesis of atrial fibrillation. *Nat Rev Cardiol*. 2015;12:230–243. doi: 10.1038/nrcardio.2015.2
27. Rosenberg MA, Das S, Pinzon PQ, Knight AC, Sosnovik DE, Ellinor PT, Rosenzweig A. A novel transgenic mouse model of cardiac hypertrophy and atrial fibrillation. *J Atr Fibrillation*. 2012;2:1–15.
28. Li N, Chiang DY, Wang S, et al. Ryanodine receptor-mediated calcium leak drives progressive development of an atrial fibrillation substrate in a transgenic mouse model. *Circulation*. 2014;129:1276–1285. doi: 10.1161/CIRCULATIONAHA.113.006611
29. Bao Y, Willis BC, Frasier CR, Lopez-Santiago LF, Lin X, Ramos-Mondragón R, Auerbach DS, Chen C, Wang Z, Anumonwo J, Valdivia HH, Delmar M, Jalife J, Isom LL. Scn2b deletion in mice results in ventricular and atrial arrhythmias. *Circ Arrhythm Electrophysiol*. 2016;9:e003923.
30. Yao C, Veleva T, Scott L, Cao S, et al. Enhanced cardiomyocyte NLRP3 Inflammasome signaling promotes atrial fibrillation [published online ahead of print May 25, 2018]. *Circulation*. https://www.ahajournals.org/doi/abs/10.1161/CIRCULATIONAHA.118.035202. doi: 10.1161/CIRCULATIONAHA.118.035202
31. Kirk JA, Chakir K, Lee KH, Karst E, Holewinski RJ, Pironti G, Tunin RS, Pozios I, Abraham TP, de Tombe P, Rockman HA, Van Eyk JE, Craig R, Farazi TG, Kass DA. Pacemaker-induced transient asynchrony suppresses heart failure progression. *Sci Transl Med*. 2015;7:319ra207. doi: 10.1126/scitranslmed.aad2899